Electronic Supplementary Material (ESI) for RSC Advances.

Supporting Information

Tb-MOF: A Naked-eye and Regenerable Fluorescent Probe for Selective and Quantitative Detection of Fe^{3+} and Al^{3+} Ions

Mengfei Zhang, ‡[a] Jing Han, ‡[a] Haipeng Wu,[a] Qing Wei,*[a] Gang Xie,[a] Sanping Chen,*[a] Shengli Gao[a]

[a] *Key Laboratory of Synthetic and Natural Functional Molecule Chemistry of Ministry of Education, College of Chemistry and Materials Science, Northwest University, Xi'an 710127, P. R. China*

‡ *These authors contributed equally to this work.*

Corresponding author

Prof. Sanping Chen

Tel.: +86-029-81535026

Fax: +86-029-81535026

E-mail: sanpingchen@126.com

Content of Table

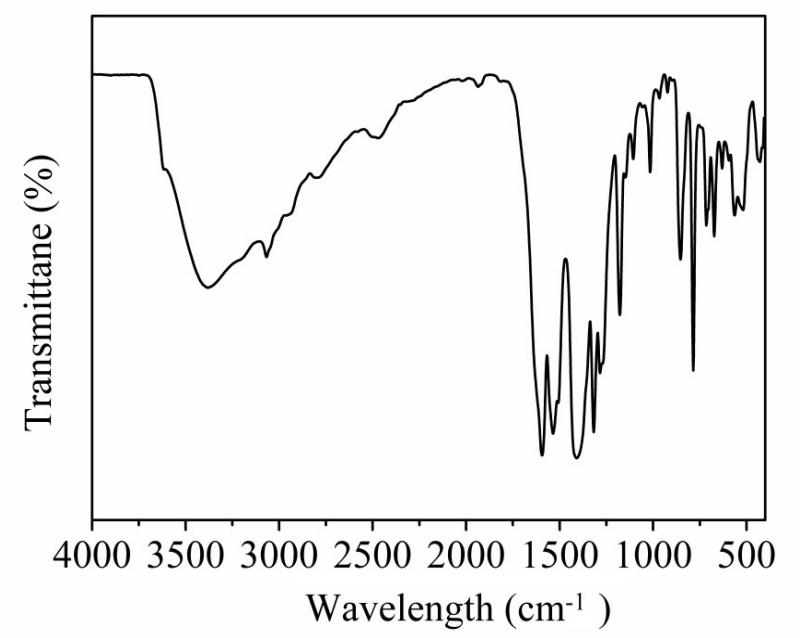

Fig. S1 FT-IR spectra of compound **1**.

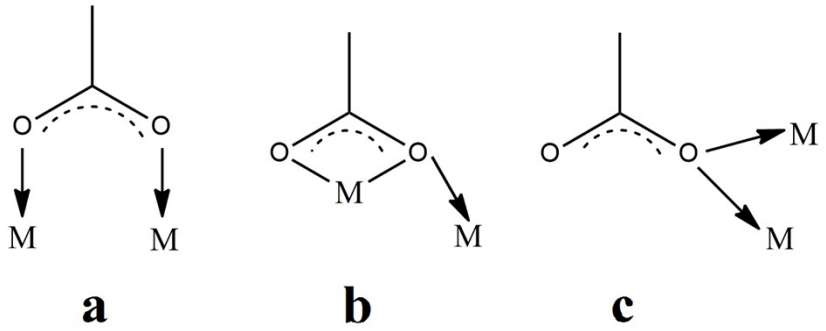

Fig. S2 The coordinated modes of TCA^{3-} ligand in compound **1**. a, μ_2-η^1:η^1; b, μ_2-η^2:η^1; c, μ_2-η^2.

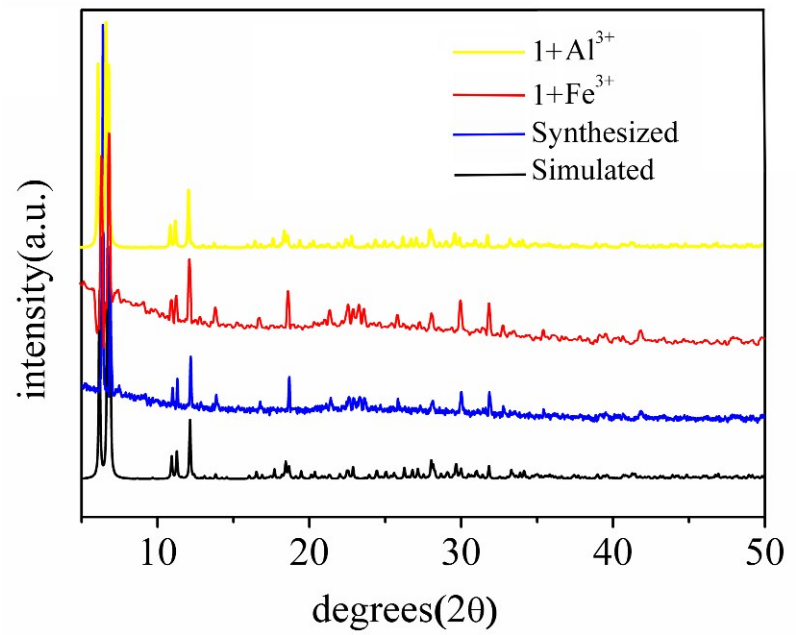

Fig. S3 Powder X-ray diffraction (PXRD) of simulated from the single-crystal data of 1 (black), as-synthesized compound **1** (blue), **1**+Fe^{3+} (red) and **1**+Al^{3+} (yellow).

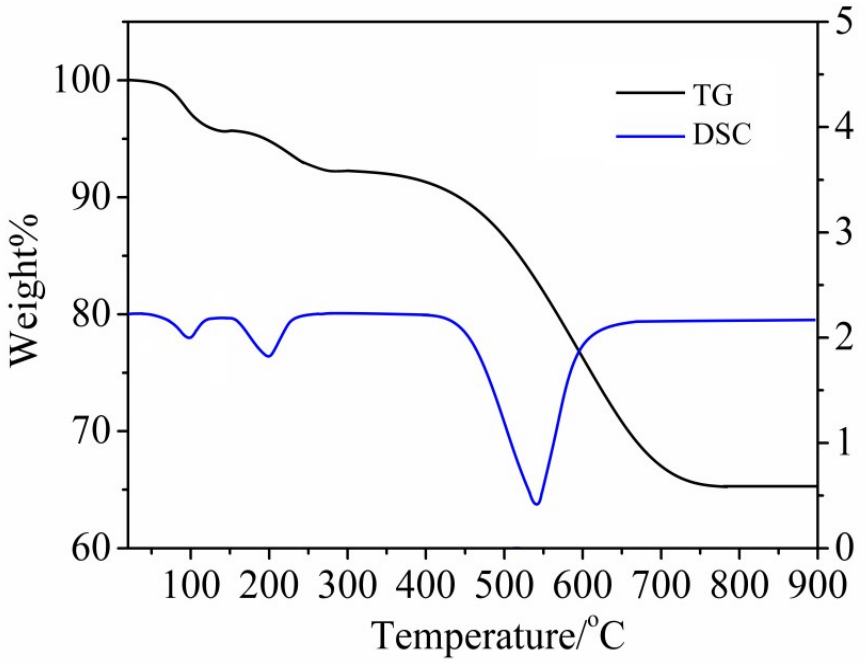

Fig. S4 Typical DSC and TG curves of compound **1**.

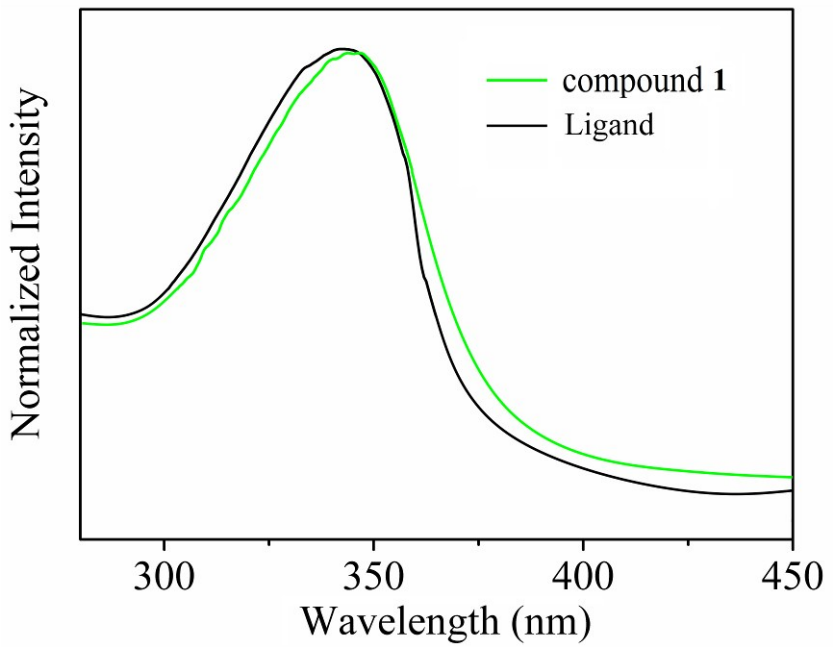

Fig. S5 The UV/vis absorption spectra of the free ligand H_3TCA and its corresponding compounds Tb-MOF were recorded in CH_3OH solution ($c = 1\times10^{-5}$ M).

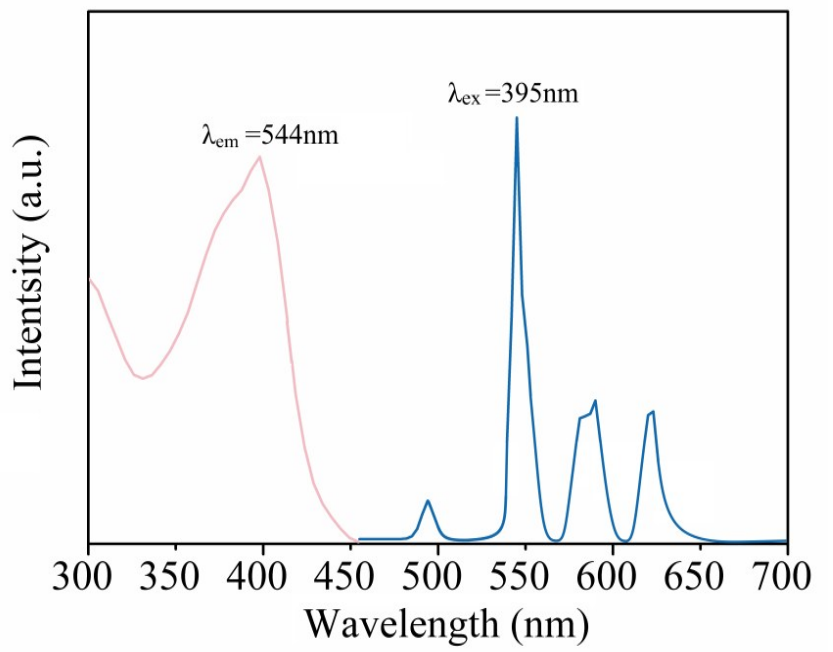

Fig. S6 Solid-state excitation (purple line) and emission (blue line) spectra of compound **1**.

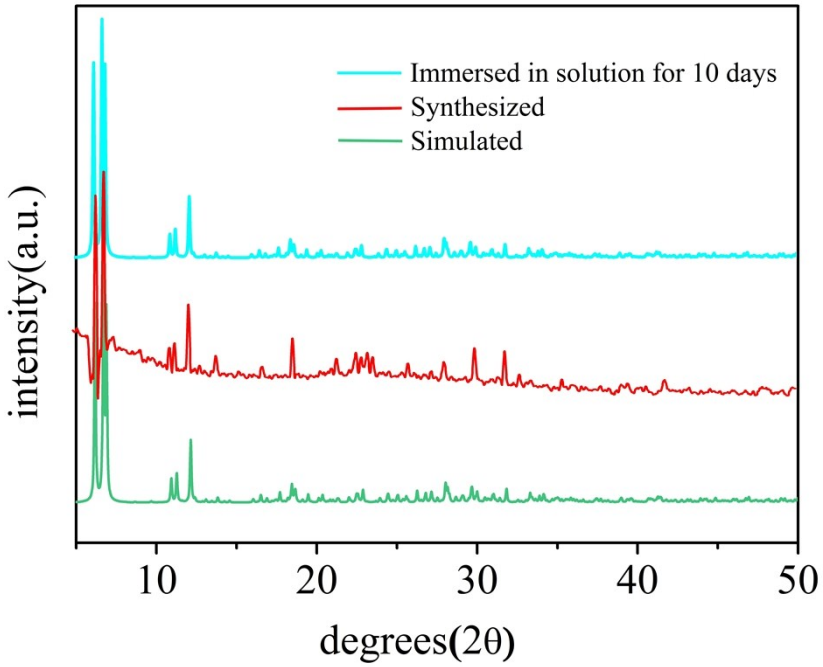

Fig. S7 PXRD patterns of Tb-MOF: the simulated pattern from single crystal analysis, as-synthesized Tb-MOF and immersed in solution for 10 days.

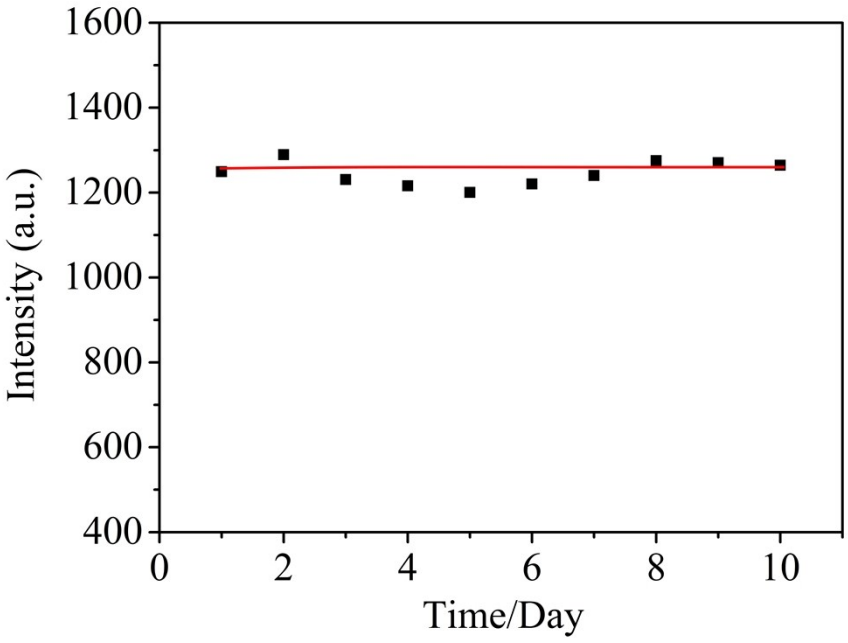

Fig. S8 Day to day fluorescence stability of compound **1** in aqueous solution.

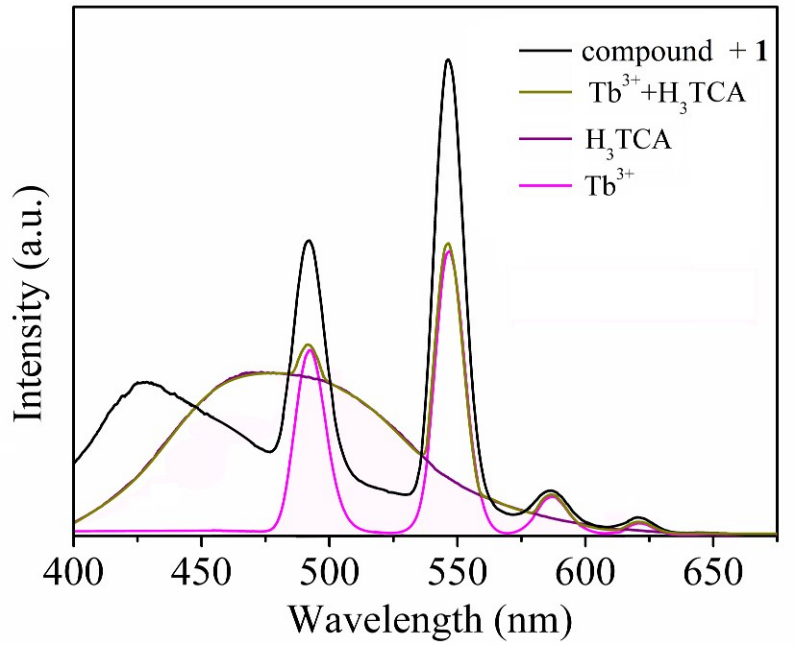

Fig. S8 Comparison of emission spectra of compound **1,** Tb^{3+} and H_3TCA (10^{-3} M) under excitation at 375 nm.

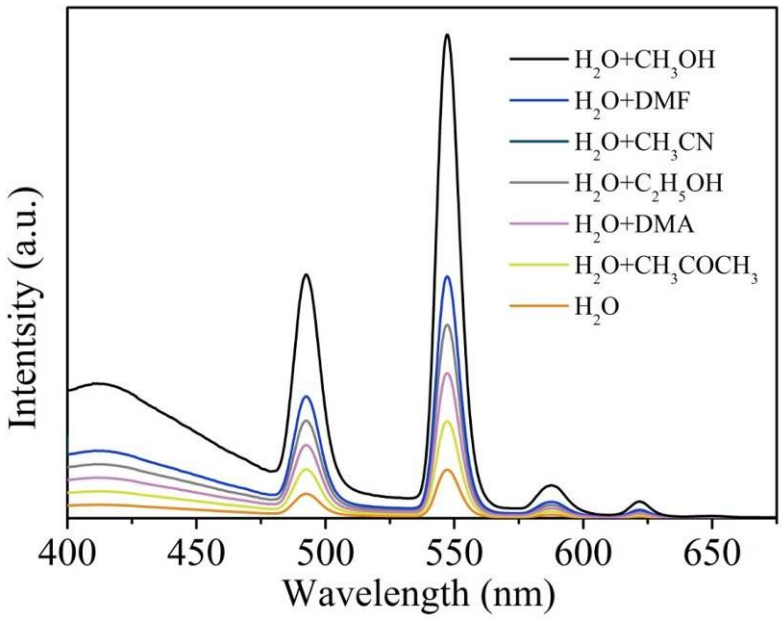

Fig. S10 Optimization of the solvent.

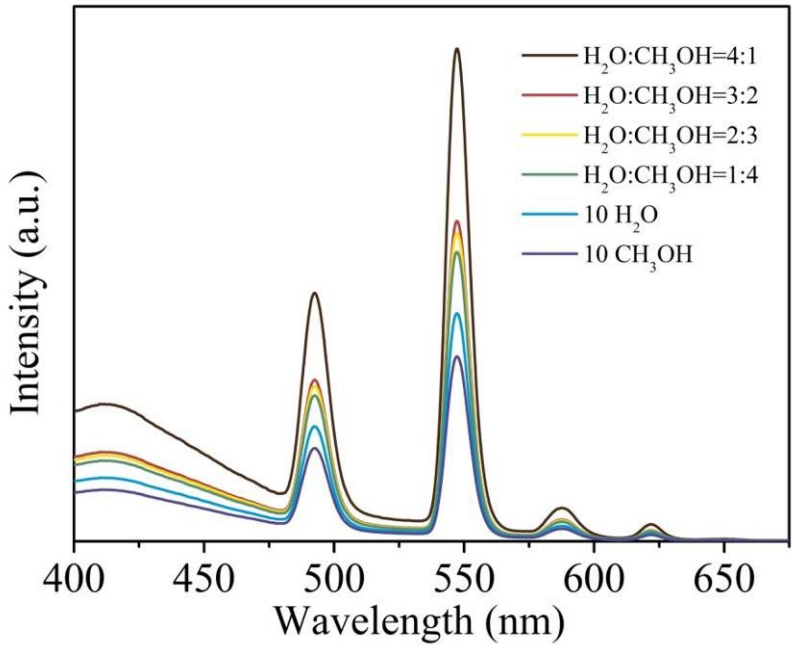

Fig. S11 Optimization of the solvent ratio.

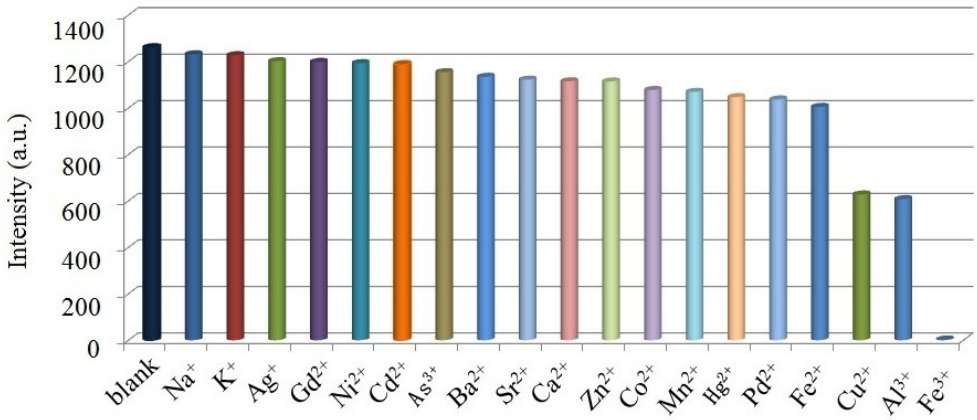

Fig. S12 Comparison of the luminescence intensity at 549 nm of compound **1** in 10^{-3} M different cations.

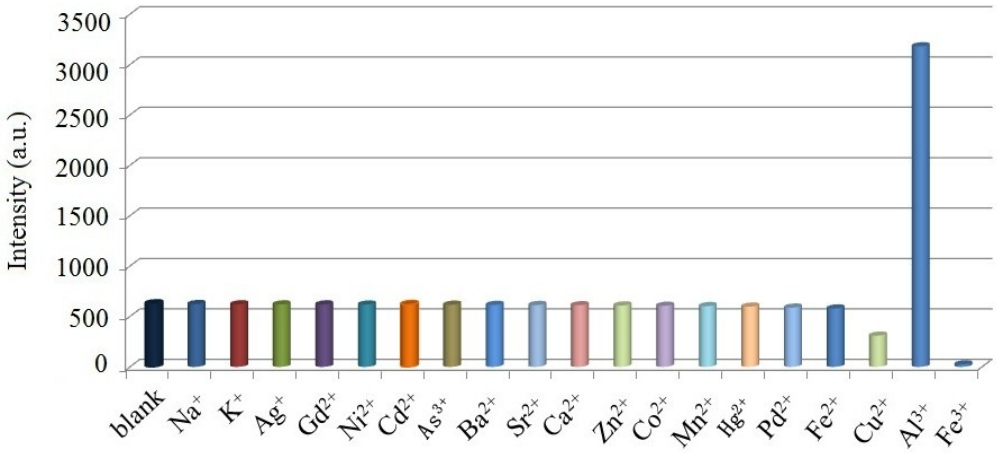

Fig. S13 Comparison of the luminescence intensity at 463 nm of compound **1** in 10^{-3} M different cations.

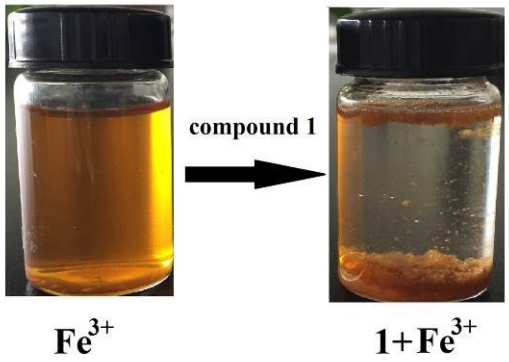

Fig. S14 Photographs showing the visual color change of the Fe^{3+} ions solution before (left) and after (right) add compound **1** about 12h.

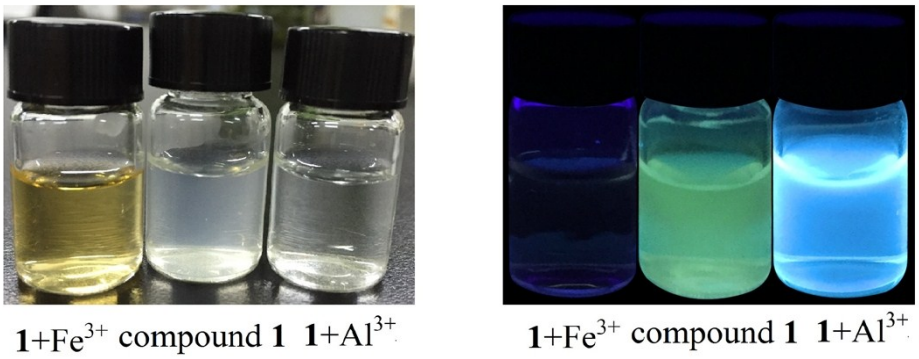

Fig. S15 The visual change on the addition of various $M(NO_3)_x$ under the fluorescent lamp (left), laboratory UV light (right, λ_{ex} = 365 nm).

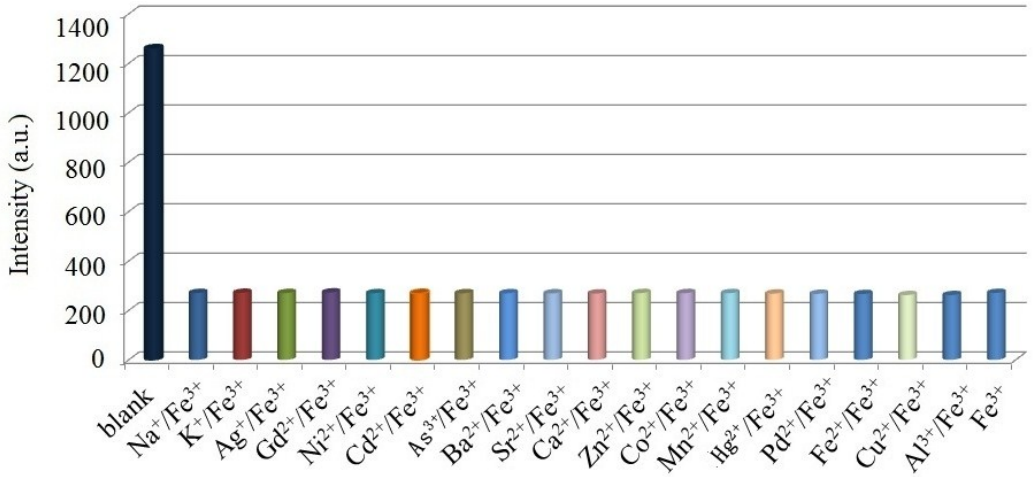

Fig. S16 Comparison of the luminescence intensity of **1**+Fe^{3+} with different metal ions at 549 nm (10^{-4} M).

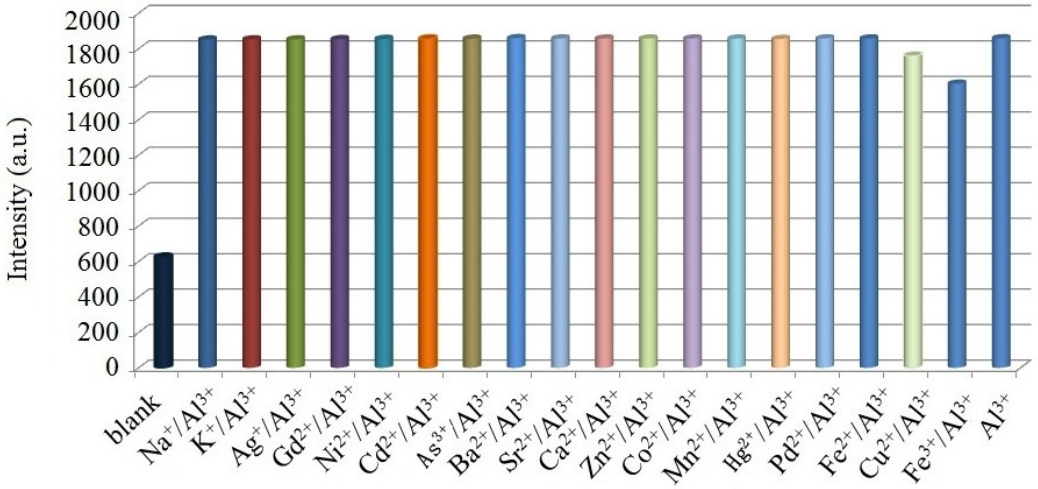

Fig. S17 Comparison of the luminescence intensity of **1**+Al^{3+} with different metal ions at 463 nm (10^{-4} M).

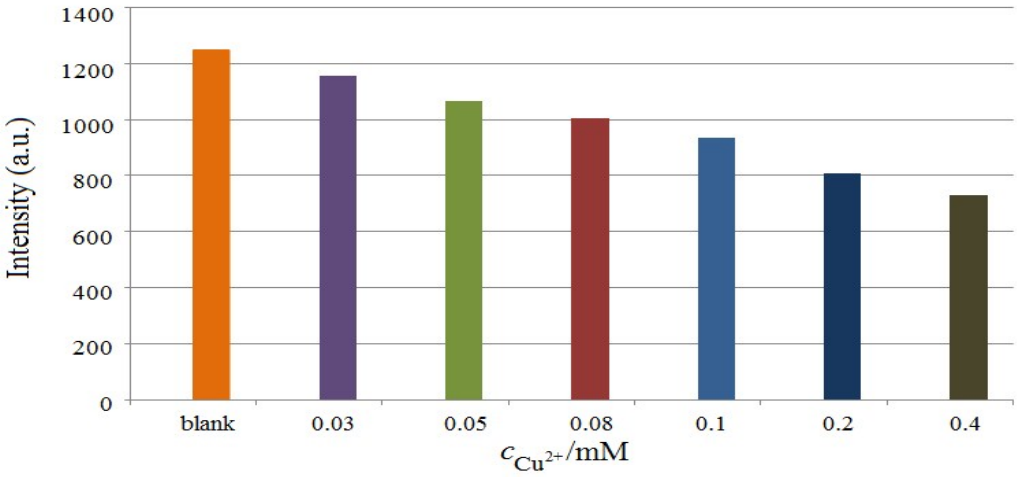

Fig. S18 Fluorescence responses of Tb-MOF in aqueous solutions in the presence of various concentrations of Cu^{2+}.

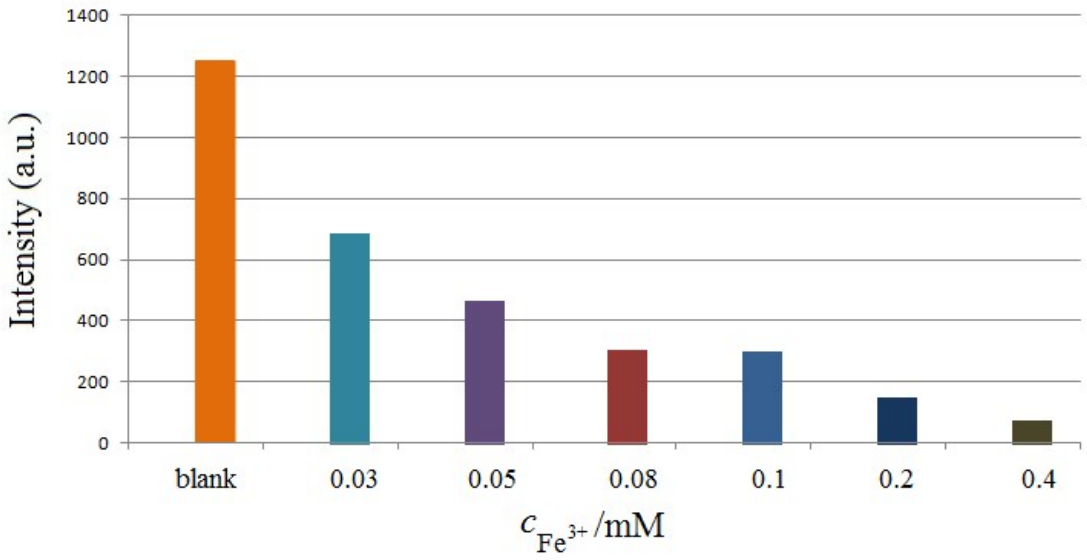

Fig. S19 Fluorescence responses of Tb-MOF in aqueous solutions in the presence of various concentrations of Fe^{3+}.

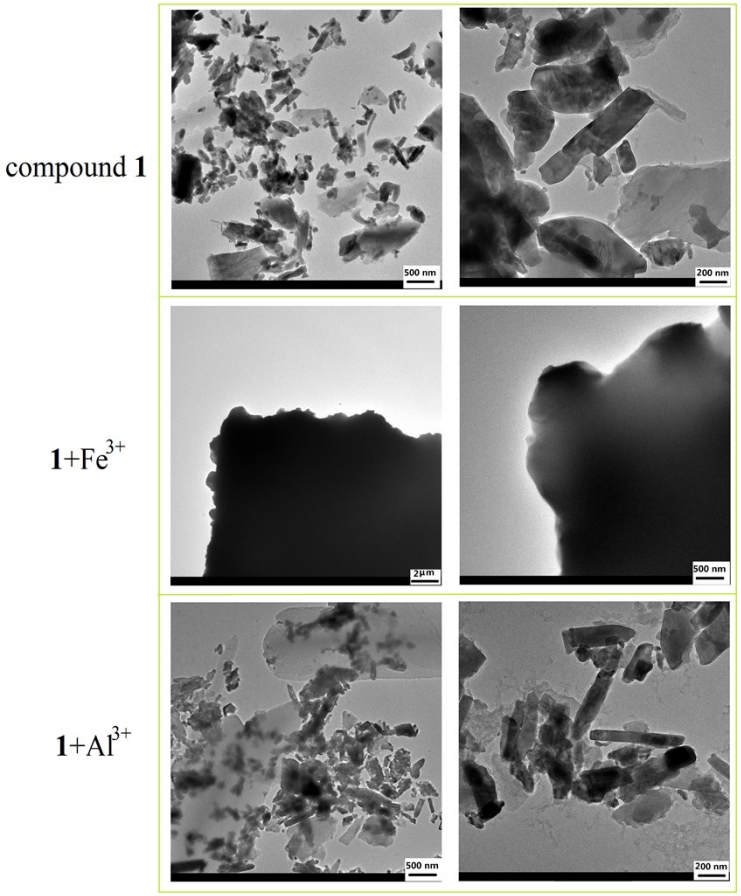

Fig. S20 Low- (right) and high- magnification (left) TEM images of the products.

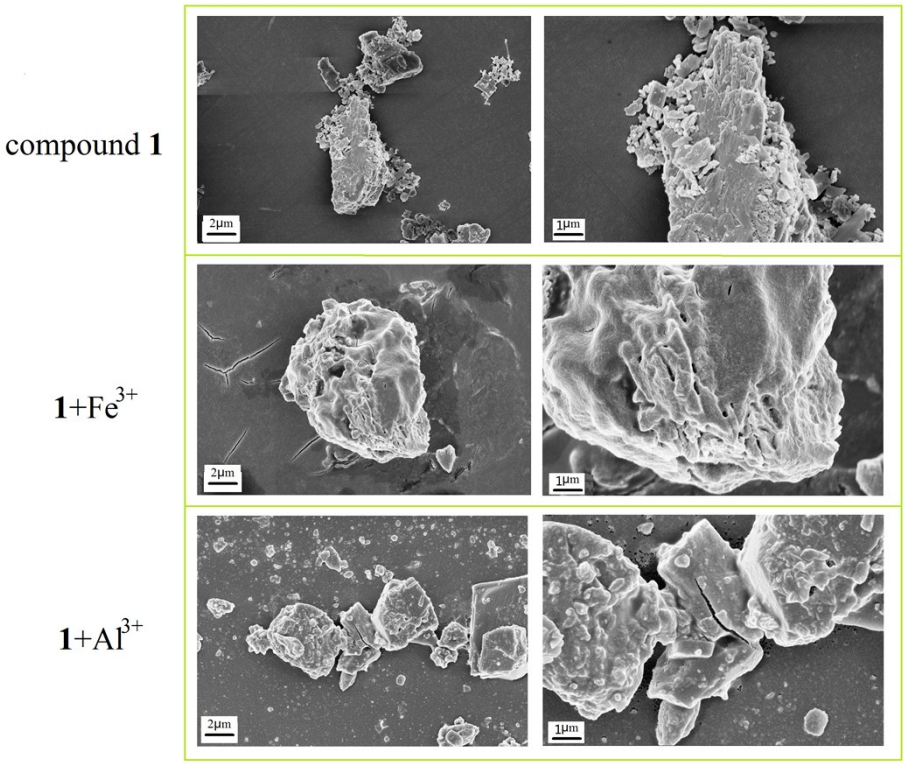

Fig. S21 Low- (right) and high- magnification (left) SEM images of the products.

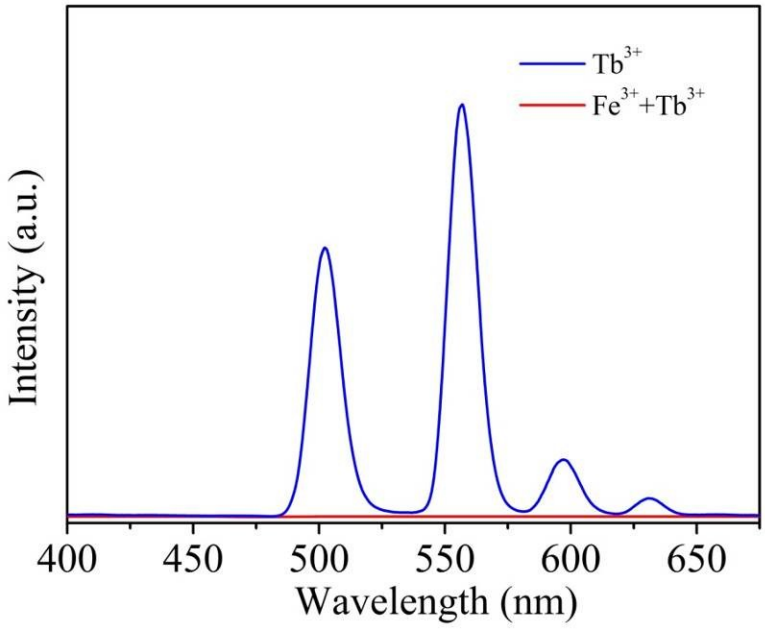

Fig. S22 Comparison of the luminescence intensity of Tb^{3+} under Fe^{3+} (10^{-3} M).

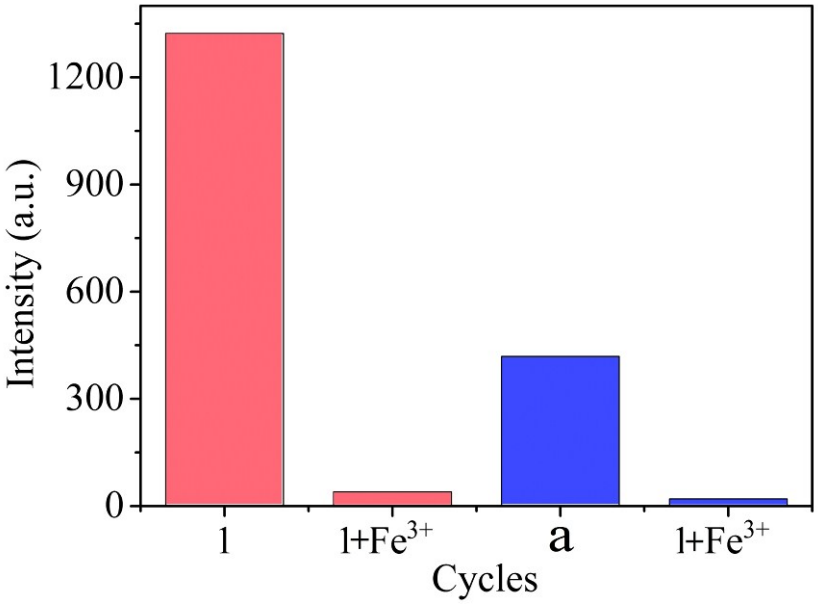

Fig. S23 The luminescence intensity (549 nm) of one recycles (a) after the first recycle.

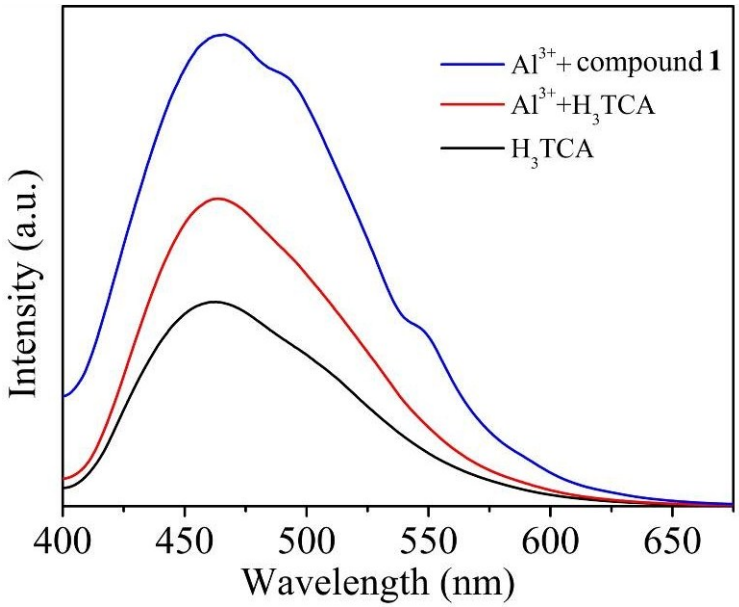

Fig. S24 Comparison of the luminescence intensity of H_3TCA and compound **1** under Al^{3+} (10^{-3} M).

Table S1. Crystal Data and Structure Refinement Summary for compound **1**.

	$[Tb_3(TCA)_2(DMA)_{0.5}(OH)_3(H_2O)_{0.5}]\cdot 3H_2O$
Empirical formula	$C_{44}H_{38.5}N_{2.5}O_{19}Tb_3$
Formula weight	1329.02
Crystal system	Monoclinic
space group	C2/c
a (Å)	29.155(3)
b (Å)	11.0593(13)
c (Å)	31.580(5)

α (deg)	90
β (deg)	115.607(2)
γ (deg)	90
V (Å^3)	9182(2)
Z	8
D_c (mg/m^3)	1.923
μ (mm^{-1})	4.643 mm^{-1}
F(000)	5095
Reflections collected/unique	24948/9386
R(int)	0.0592
Data / restraints / parameters	9386/42/623
Goodness-of-fit on F^2	1.01
R1[a] [I>2sigma(I)]	0.0422
wR$_2$[b] (all data)	0.1097

[a]$R_1 = \Sigma(F_o - F_c)/\Sigma F_o$. [b]$wR_2 = [\Sigma w(F_o^2 - F_c^2)^2/\Sigma w(F_o^2)^2]^{1/2}$[a].

Table S2. Selected Bond Lengths (Å) and Bond Angles (o) for compound **1**.

Tb1-O1^3	2.772(5)	O14^2-Tb1-O5^4	156.01(18)
Tb1-O2^3	2.427(5)	O14^2-Tb1-O6^4	131.56(18)
Tb1-O3	2.512(5)	O14^2-Tb1-O9^1	99.59(17)
Tb1-O4	2.331(6)	O15^2-Tb1-O1^3	131.27(16)
Tb1-O5^4	2.443(6)	O15^2-Tb1-O2^3	128.6(2)
Tb1-O6^4	2.427(6)	O15^2-Tb1-O3	72.30(17)
Tb1-O9^1	2.404(5)	O15^2-Tb1-O5^4	127.27(18)
Tb1-O14^2	2.390(5)	O15^2-Tb1-O6^4	138.94(19)
Tb1-O15^2	2.349(5)	O15^2-Tb1-O9^1	69.68(17)
Tb2-O3^6	2.389(5)	O15^2-Tb1-O14^2	66.67(17)
Tb2-O5^7	2.630(6)	O3^5-Tb2-O5^7	62.15(18)
Tb2-O8	2.314(5)	O3^5-Tb2-O9^8	81.14(18)
Tb2-O9	2.389(5)	O3^5-Tb2-O9	77.22(17)
Tb2-O9^8	2.431(5)	O3^5-Tb2-O10	80.3(2)
Tb2-O10	2.459(6)	O3^5-Tb2-O13^7	134.79(17)
Tb2-O13^7	2.910(6)	O3^5-Tb2-O16^7	92.67(19)
Tb2-O15^7	2.349(5)	O8-Tb2-O3^5	128.71(19)
Tb2-O16^7	2.413(6)	O8-Tb2-O5^7	66.60(18)
Tb3-O1^7	2.387(5)	O8-Tb2-O9	83.7(2)
Tb3-O7^7	2.304(5)	O8-Tb2-O9^8	133.38(19)
Tb3-O11^9	2.372(6)	O8-Tb2-O10	140.8(2)
Tb3-O1^3	2.294(5)	O8-Tb2-O13^7	70.75(19)
Tb3-O14^{10}	2.389(5)	O8-Tb2-O15^7	72.45(19)
Tb3-O14	2.357(5)	O8-Tb2-O16^7	78.0(2)
Tb3-O15	2.325(5)	O9^8-Tb2-O5^7	128.20(16)
O2^3-Tb1-O1^3	49.70(17)	O9-Tb2-O5^7	69.33(17)

$O2^{3}$-Tb1- O3	136.63(18)	O9-Tb2-$O9^{8}$	67.7(2)
$O2^{3}$-Tb1-$O5^{4}$	76.2(2)	$O9^{8}$-Tb2-O10	68.33(19)
$O2^{3}$-Tb1-$O6^{4}$	92.4(2)	O9-Tb2-O10	133.0(2)
O3-Tb1-$O1^{3}$	149.49(17)	$O9^{8}$-Tb2-$O13^{7}$	116.28(16)
O4-Tb1-$O1^{3}$	77.11(19)	O9-Tb2-$O13^{7}$	147.36(16)
O4-Tb1-$O2^{3}$	126.3(2)	O9-Tb2-$O16^{7}$	146.43(19)
O4-Tb1-O3	92.21(19)	O10-Tb2-$O5^{7}$	131.6(2)
O4-Tb1-$O5^{4}$	127.82(19)	O10-Tb2-$O13^{7}$	70.14(19)
O4-Tb1-$O6^{4}$	76.6(2)	$O15^{7}$-Tb2-$O3^{5}$	149.56(19)
O4-Tb1-$O9^{1}$	148.0(2)	$O15^{7}$-Tb2-$O5^{7}$	133.30(17)
O4-Tb1-$O14^{2}$	70.51(18)	$O15^{7}$-Tb2-$O9^{8}$	69.21(17)
O4-Tb1-$O15^{2}$	78.6(2)	$O15^{7}$-Tb2-O9	85.10(17)
$O5^{4}$-Tb1-$O1^{3}$	100.86(18)	$O15^{7}$-Tb2-O10	94.5(2)
$O5^{4}$-Tb1-O3	63.24(18)	$O15^{7}$-Tb2-$O13^{7}$	68.33(16)
$O6^{4}$-Tb1-$O1^{3}$	73.23(18)	$O16^{7}$-Tb2-$O5^{7}$	77.60(19)
$O6^{4}$-Tb1-O3	76.53(19)	$O16^{7}$-Tb2-$O9^{8}$	143.01(18)
$O6^{4}$-Tb1-$O5^{4}$	54.06(18)	$O16^{7}$-Tb2-O10	74.7(2)
$O9^{1}$-Tb1-$O1^{3}$	127.72(16)	$O16^{7}$-Tb2-$O13^{7}$	47.47(18)
$O9^{1}$-Tb1-$O2^{3}$	74.64(16)	$O1^{7}$-Tb3-$O14^{10}$	72.19(19)
$O9^{1}$-Tb1-O3	79.17(18)	$O7^{7}$-Tb3-O17	80.47(19)
$O9^{1}$-Tb1-$O5^{4}$	72.37(18)	$O7^{7}$-Tb3-$O1^{19}$	78.4(2)
$O9^{1}$-Tb1-$O6^{4}$	126.10(18)	$O7^{7}$-Tb3-O14	143.03(18)
$O14^{2}$-Tb1-$O1^{3}$	65.59(17)	$O7^{7}$-Tb3-$O14^{10}$	136.15(18)
$O14^{2}$-Tb1-$O2^{3}$	80.1(2)	$O7^{7}$-Tb3-O15	76.57(19)
$O14^{2}$-Tb1-O3	137.72(18)		